Theory of electron Zitterbewegung in graphene probed by femtosecond laser pulses

Tomasz M. Rusin[1,*] and Wlodek Zawadzki[2]
[1]*PTK Centertel Sp. z o.o., ul. Skierniewicka 10A, 01-230 Warsaw, Poland*
[2]*Institute of Physics, Polish Academy of Sciences, Al. Lotników 32/46, 02-688 Warsaw, Poland*
(Received 27 December 2008; published 16 July 2009)

We propose an experiment allowing an observation of Zitterbewegung (ZB, trembling motion) of electrons in graphene in the presence of a magnetic field. In contrast to the existing theoretical work we make no assumptions concerning shape of the electron wave packet. A femtosecond Gaussian laser pulse excites electrons from the valence $n=-1$ Landau level into three other levels, creating an oscillating electron wave packet with interband and intraband frequencies. Oscillations of an average position of the packet are directly related to the induced dipole moment and oscillations of the average packet's acceleration determine emitted electric field. Both quantities can be measured experimentally. A broadening of Landau levels is included to make the description of ZB as realistic as possible. Criteria of realization of a ZB experiment are discussed.

DOI: 10.1103/PhysRevB.80.045416 PACS number(s): 73.22.−f, 73.63.Fg, 78.67.Ch, 03.65.Pm

I. INTRODUCTION

Zitterbewegung (ZB, trembling motion) of relativistic electrons in a vacuum was predicted nearly 80 years ago by Schrodinger.[1] Unfortunately, both the spacial extension of the ZB motion, being of the order of $\lambda_c=\hbar/mc$, and the ZB frequency $\omega_Z=2mc^2/\hbar$ are far beyond current experimental possibilities. However, it was recently shown that, because of an analogy between the behavior of relativistic electrons in a vacuum and that of electrons in narrow gap semiconductors,[2,3] one can expect the trembling motion of electrons in narrow gap semiconductors having much more advantageous characteristics: the frequency $\omega_Z=E_g/\hbar$ and the amplitude $\lambda_Z=\hbar/m_0^*u$, where E_g is the energy gap, m_0^* is the electron effective mass, and $u=(E_g/2m_0^*)^{1/2}$ is the maximum electron velocity in the two-band energy spectrum.[4] It was further shown that the ZB-like motion should occur in other two-band situations, both in solids[5–18] and in other systems.[19–26] An observation of an acoustic analogue of ZB was reported recently in sonic crystals.[27]

It was predicted some time ago by Lock[28] that, if an electron is represented by a wave packet, the ZB phenomenon will have a transient character. This was confirmed by very recent calculations which predicted that the decay times of ZB are of the order of femtoseconds to microseconds depending on the system in question.[12,16,21] However, it was also shown that the presence of an external magnetic field and the resulting Landau quantization of the electron spectrum "stabilizes" the situation making the ZB oscillations stationary in time, if one neglects the loss of electron energy due to dipole radiation.[15,29] It is known that an external magnetic field does not induce interband electron transitions, so that an interference of electron states corresponding to positive and negative energies remains unchanged and an appearance of interband frequencies remains the signature of ZB phenomenon. On the other hand, due to Landau quantization of the electron and hole energies also intraband (cyclotron) excitations appear in the spectrum.

All the recent theoretical work on ZB assumed that initially the electrons are represented by Gaussian wave packets.[6,12,15,21–24,28,30] While this assumption represents a real progress compared to the initial work that had treated electrons as plain waves,[5,4,7–9,11,19,31,32] it is obviously an idealization since it is not quite clear how to prepare an electron in this form. It is the purpose of our present work to propose and describe an observation of electron ZB in semiconductors that can be really carried out. Namely, we calculate a reaction of an electron in graphene excited by a laser pulse, not assuming anything about initial form of the electron wave packet. In our description we take into account currently available experimental possibilities. Also, we include a broadening of Landau levels and investigate its effect on the trembling motion. It is our hope that this proposition will help to observe this somewhat mysterious effect that is fundamental for both relativistic electrons in a vacuum and electrons in narrow gap semiconductors.

The following conditions should be met for a successful observation of ZB: (a) The ZB frequency must be in the range of currently detectable regimes, i.e., of the order of $\omega_Z\approx 1$ fs^{-1}, and the size of oscillations should be of the order of a few Å; (b) the ZB oscillations should be persistent or slowly transient; (c) both positive and negative electron energies must be excited with a sufficient probability; (d) to avoid many-electron effects (see Refs. 33 and 34), the wave packet should be created in a one-electron regime. A system that in our opinion fulfills the above criteria is *p*-type monolayer graphene in a constant magnetic field. The wave packet should be created by an ultra short monocycle or submonocycle laser pulse. Because of a very wide frequency spectrum of such a pulse, the resulting wave packet will have both positive and negative energies. The electron oscillations give rise to a time-dependent dipole moment which will be a source of electric field and it will emit or absorb radiation in the far infrared range. Experimental parameters necessary to create the optical wave packet and to detect the radiation should be within the current experimental possibilities.

Our paper is organized as follows. In Secs. II and III we calculate the electron reaction to a short laser pulse, the creation of ZB and we describe an electric field of radiation emitted by the trembling electron. In Sec. IV the influence of Landau level broadening on the trembling motion is investigated. In Sec. V we describe the time-dependent luminescence filtered by a time gate and a frequency filter. Finally, we discuss our results and conclude by a summary.

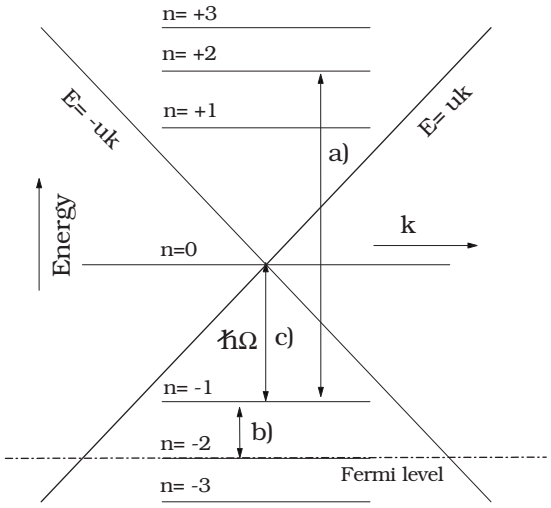

FIG. 1. Electron energy levels for monolayer graphene in a magnetic field. Proposed position of the Fermi level is indicated. Arrows show interband (a), intraband (b), and fundamental (c) energies, see text.

II. PRELIMINARIES

We consider p-type monolayer graphene in the presence of a magnetic field perpendicular to the layer. The electron-hole Hamiltonian $\hat{H}_1$ at the K_1 point of the Brillouin zone is given by[35–37]

$$\hat{H}_1 = -\hbar\Omega\begin{pmatrix} 0 & \hat{a} \\ \hat{a}^+ & 0 \end{pmatrix}, \tag{1}$$

where $\hat{a}$, $\hat{a}^+$ are the lowering and rising operators and the characteristic frequency of the system is $\Omega=\sqrt{2}u/L$, where $L=\sqrt{\hbar/eB}$ is the magnetic length and the velocity $u \simeq 10^8$ cm/s. The energy spectrum of $\hat{H}_1$ is $E_n = \mathrm{sgn}(n)\hbar\Omega\sqrt{|n|}$, where $n=0,\pm 1,\ldots$, see Fig. 1. The eigenstates of Hamiltonian (1) for the gauge $\boldsymbol{A}=[-By,0,0]$ are

$$\psi_n(\boldsymbol{r}) = \frac{e^{ik_x x}}{\sqrt{4\pi}}\begin{pmatrix} -\mathrm{sgn}(n)\phi_{|n|-1}(\xi) \\ \phi_{|n|}(\xi) \end{pmatrix}, \tag{2}$$

where $\xi=y/L-k_xL$ and $\phi_n(\xi)=(C_n/\sqrt{L})e^{-1/2\xi^2}\mathrm{H}_n(\xi)$ is the n-th eigenstate of the harmonic oscillator. Here $C_n = 1/\sqrt{2^n n!\sqrt{\pi}}$ and $\mathrm{H}_n(\xi)$ are the Hermite polynomials. For $n=0$, the first component in Eq. (2) vanishes and the normalization coefficient is $1/\sqrt{2\pi}$. We assume the Fermi level to coincide with the Landau level (LL) $n=-2$ and consider the initial electron in $n=-1$ state, see the Discussion below.

The wavelength of the laser light is assumed to be much larger than the spacial size L of the $n=-1$ state, so we can neglect spacial variation of the electric field in the laser pulse. We take the perturbing potential due laser light in the form

$$\hat{W}(t) = -ey\mathcal{E}_0 e^{-(2\ln 2)t^2/\tau^2}\cos(\omega_L t), \tag{3}$$

where e is the electron charge, τ is the pulse duration (FWHM), $\omega_L=2\pi c/\lambda_L$ is the laser frequency (being of the order of 3×10^{15} s^{-1}), and $\mathcal{E}_0$ is the amplitude of electric field. A Gaussian shape of the laser pulse is widely used in optical experiments and it parameterizes effectively a profile of electric field in the laser beam.

As a result of a laser shot, the initial state of the system $\Phi_k(t)=\psi_k e^{-iE_k t/\hbar}$ evolves into the final state $\Psi_k(t) = \Sigma_j c_j(t)\psi_k e^{-iE_j t/\hbar}$, which is a combination of the eigenstates of $\hat{H}_1$ with suitably chosen coefficients $c_j(t)$. The resulting time-dependent dipole moment is $\boldsymbol{D}(t)=e\langle\Psi_k(t)|\boldsymbol{r}|\Psi_k(t)\rangle$.

The total Hamiltonian, including the perturbation due to the laser light, is

$$\hat{H} = \hat{H}_1 + \hat{W}(t). \tag{4}$$

The corresponding time-dependent wave functions are $\Psi_k(t)=e^{-i\hat{H}t/\hbar}\Psi_k(0)$, and the dipole moment is

$$\begin{aligned}\boldsymbol{D}(t) &= e\langle\Psi_k(0)e^{i\hat{H}t/\hbar}|\hat{\boldsymbol{r}}|e^{-i\hat{H}t/\hbar}\Psi_k(0)\rangle \\ &= e\langle\Psi_k(0)|\hat{\boldsymbol{r}}(t)|\Psi_k(0)\rangle = e\langle\boldsymbol{r}(t)\rangle.\end{aligned} \tag{5}$$

Here $\boldsymbol{r}(t)$ is the electron position in the Heisenberg picture. Thus the dipole moment $\boldsymbol{D}(t)$ is proportional to the time-dependent position averaged over the electron wave packet.

A time-dependent dipole moment is a source of electromagnetic radiation. We treat the radiation classically[38] and take the radiated transverse electric field to be[39]

$$\mathcal{E}_\perp(\boldsymbol{r},t) = \frac{\ddot{\boldsymbol{D}}(t)}{4\pi\epsilon_0 c^2}\frac{\sin(\theta)}{R}, \tag{6}$$

where ϵ_0 is the vacuum permittivity, θ is an angle between the direction of electron motion and a position of the observer $\boldsymbol{R}$. Since $\ddot{\boldsymbol{D}}(t)=e\langle\ddot{\boldsymbol{r}}(t)\rangle$, Eq. (6) relates the electric field of the dipole with the average acceleration of the packet. If the electric field is measured directly by an antenna, one measures the trembling motion of the wave packet. If the square of electric field is measured in emission or absorption experiments, the signature of ZB is the existence of peaks corresponding to interband and intraband frequencies and their dependence on packet's parameters. Accordingly, in the time resolved luminescence experiments it should be possible to detect directly the motion of the packet with interband and intraband frequencies.

III. EMITTED ELECTRIC FIELD

Now we calculate explicitly the electric field emitted by the trembling electron. If we consider the perturbation of Eq. (4), the standard time-dependent perturbation theory gives for the wave function[40]

$$\Psi_n(t) \simeq \psi_n e^{-iE_n t/\hbar} + \sum_j c^1_{nj}(t)\psi_j e^{-iE_j t/\hbar} + \ldots, \tag{7}$$

with

$$c^1_{nj}(t) = \frac{1}{i\hbar}\int_{-\infty}^{t}\hat{W}_{nj}(t')e^{i(E_n-E_j)t'/\hbar}dt'. \tag{8}$$

Setting the initial state to be $n=-1$ and using Eq. (3) we have

$$c^1_{-1j}(t) = -\frac{1}{i}\left(\frac{\sqrt{\pi}eL\mathcal{E}_0\tau}{\hbar\sqrt{\alpha}}\right)a^y_{-1j}b_{-1j}(t), \tag{9}$$

where

$$a^y_{-1j} = \frac{1}{L}\int \psi^\dagger_{-1}(\boldsymbol{r})y\psi_j(\boldsymbol{r})d\boldsymbol{r}, \tag{10}$$

$$b_{-1j}(t) = \frac{\sqrt{\alpha}}{\sqrt{\pi}\tau}\int_{-\infty}^{t} e^{-\alpha t'^2/\tau^2}e^{i\omega_{-1j}t'}\cos(\omega_L t')dt'. \tag{11}$$

Here $\omega_{-1j}=(E_{-1}-E_j)/\hbar$ and $\alpha=2\ln 2\approx 1.34$. Since the size of $n=-1$ state is of the order of L, the coefficients a^y_{-1j} are of the order of unity. It is also is easy to show that $|b_{-1j}|\leq 1$. The dimensionless perturbation expansion parameter is $\zeta=\sqrt{\pi}eL\mathcal{E}_0\tau/\hbar\sqrt{\alpha}$.

To obtain the coefficients a_{-1j} from Eq. (10) we calculate the matrix elements of y between different eigenstates $\psi_n(\boldsymbol{r})$ of $\hat{H}_1$. The selection rules for $\langle\psi_n|y|\psi_j\rangle$ of Eq. (10) are $|n|-|j|=\pm 1$, so for $n=-1$ there are three nonvanishing matrix elements corresponding to $j=0,\pm 2$, see Fig. 1. The approximate wave function $\Psi_{-1}(t)$ is then

$$\Psi_{-1}(t) \simeq e^{-iE_{-1}t/\hbar}\psi_{-1} + \sum_{j=0,\pm 2} c^1_{-1j}e^{-iE_jt/\hbar}\psi_j. \tag{12}$$

Therefore, the laser shot creates a nonstationary wave packet given by Eq. (12). This wave packet contains states with positive and negative energies, which is a necessary condition to create the ZB motion.[6,12] If the packet contains only positive or only negative energy states, the ZB will not occur. To calculate $\boldsymbol{D}(t)$, we average $\hat{y}$ and $\hat{x}$ over the wave function (12). As a result we obtain 16 terms, of which one term does not depend on c_{-1j}, six terms are proportional to c_{-1j}, and the remaining nine terms are of the second order in c_{-1j}. Since the zero order term does not depend on time, we concentrate on the time-dependent terms of the lowest order in $\mathcal{E}_0$, and we have

$$D_y(t) \simeq \text{const} + eL\sum_{j=0,\pm 2} c^1_{-1j}a^y_{-1j}e^{i\omega_{-1j}t} + \text{H.c.} + \ldots, \tag{13}$$

and similarly for $D_x(t)$, with a^y_{-1j} replaced by a^x_{-1j}. Because the pulse duration τ is much shorter than the period of ZB oscillations $T_Z\approx 2\pi/\Omega$, we approximate $b_{-1j}(t)$ by $b_{-1j}(\infty)$. Then [see Eq. (11)]

$$b_{-1j} \approx b_{-1j}(\infty) = \frac{1}{2}\sum_{s=\pm 1} e^{-(\omega_{-1j}+s\omega_L)^2\tau^2/4\alpha}. \tag{14}$$

Within this approximation we have

$$D_y(t) = d_0\left[-\frac{b_{-10}}{2}\sin(\omega^c_0 t) + B^- b_{-12}\sin(\omega^Z_1 t) + B^+ b_{-1-2}\sin(\omega^c_1 t)\right],$$

$$D_x(t) = d_0\left[\frac{b_{-10}}{2}\cos(\omega^c_0 t) + B^- b_{-12}\cos(\omega^Z_1 t) - B^+ b_{-1-2}\cos(\omega^c_1 t)\right], \tag{15}$$

where $\omega^c_n=\Omega(\sqrt{n+1}-\sqrt{n})$, $\omega^Z_n=\Omega(\sqrt{n+1}+\sqrt{n})$, $B^\pm=\sqrt{2}/2\pm 3/4$, and $d_0=-eL\zeta$. Taking the second time derivative of the dipole moment we find the electric field components of the emitted electromagnetic wave

$$\mathcal{E}_y(\boldsymbol{r},t) = \Xi(\boldsymbol{r})\left[\frac{b_{-10}}{2}\sin(\omega^c_0 t) + \frac{b_{-12}}{4}\sin(\omega^Z_1 t) - \frac{b_{-1-2}}{4}\sin(\omega^c_1 t)\right],$$

$$\mathcal{E}_x(\boldsymbol{r},t) = \Xi(\boldsymbol{r})\left[-\frac{b_{-10}}{2}\cos(\omega^c_0 t) + \frac{b_{-12}}{4}\cos(\omega^Z_1 t) + \frac{b_{-1-2}}{4}\cos(\omega^c_1 t)\right], \tag{16}$$

where $\Xi(\boldsymbol{r})=d_0\Omega^2\sin(\theta)/(4\pi\epsilon_0 c^2R^2)$. Equations (15) and (16) are among the main results of our work. They state that both the induced dipole moment and the corresponding electric field oscillate with three frequencies. The frequency $\omega_{-12}=(\sqrt{2}+1)\Omega$ corresponds to the Zitterbewegung, i.e., to the motion of the packet with an interband frequency. This frequency corresponds to the interband ZB frequency $\omega_Z=2m_ec^2/\hbar$ of relativistic electrons in a vacuum. The interband frequency is characteristic of ZB because the trembling motion occurs due to an interference of electron states related to positive and negative electron energies.[31,32] The second frequency $\omega_{-1-2}=(\sqrt{2}-1)\Omega$ describes the intraband cyclotron motion of the packet. The third frequency $\omega_{-10}=\Omega$ has both interband and intraband character (see Fig. 1). Contrary to the relativistic quantum mechanics, in zero-gap materials such as graphene, the interband ZB frequency is not vastly larger than the cyclotron frequency.

In Fig. 2 we plot the oscillating dipole moment within the first 1000 fs of motion after the laser shot for two magnetic fields $B=1$ T and $B=10$ T, and two laser pulses. The first pulse [Figs. 2(a) and 2(b)] has a duration $\tau=1.6$ fs and a base laser wavelength $\lambda_L=650$ nm. This pulse has a submonocycle duration and it is the shortest pulse created experimentally within the visible laser wavelength.[41] In Figs. 2(c) and 2(d) we assume pulse duration $\tau=3.0$ fs and a laser wavelength $\lambda_L=720$ nm. This pulse has 1.25 of the laser monocycle and its experimental properties were discussed in Ref. 42. The use of a few monocycle pulses (with $\tau>5$ fs) is not effective, since the probability of excitation of a wave packet in Eq. (12) drops exponentially with pulse duration τ, see Eq. (14).

In Fig. 3 we plot the corresponding electric field for the same parameters during the first 250 fs of oscillations. We assume the laser intensity to be $I=1.0\times 10^9$ W/cm^2, the emitted electromagnetic wave detected at the angle $\theta=45°$, and the distance $R=1$ cm. All the quantities in Figs. 2 and 3 are calculated per one electron. Since the frequencies are incommensurable, the electron trajectories $\boldsymbol{r}(t)$ are not closed and there is no repeated pattern of oscillations. The motion of the wave packet is permanent in the time scale of femto-

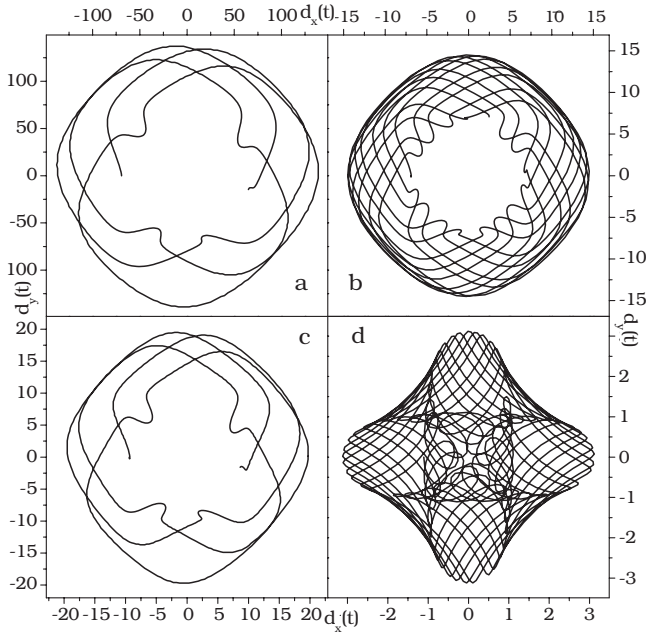

FIG. 2. Oscillations of dipole moment during the first 1000 fs of electron motion after the laser pulse. Experimental characteristics: pulse intensity 1×10^9 W/cm^2, (a) τ=1.6 fs, B=1 T, (b) τ=1.6 fs, B=10 T, (c) τ=3.0 fs, B=1 T, and (d) τ=3.0 fs, B=10 T. Dipole moments in (a) and (b) are in 10^{-28} [Cm] units, while in (c) and (d) they are in 10^{-31} [Cm] units. The above results refer to very narrow Landau levels, disregarding broadening due to electron scattering and the e-e interaction, see Sec. IV.

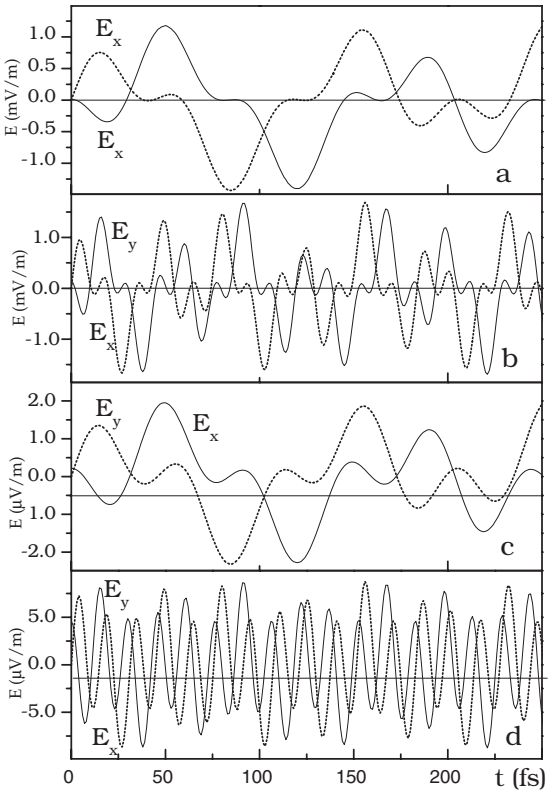

FIG. 3. Electric field emitted by one electron during the first 250 fs of electron motion after the laser pulse. Experimental characteristics: pulse intensity 1×10^9 W/cm^2, (a) τ=1.6 fs, B=1 T, (b) τ=1.6 fs, B=10 T, (c) τ=3.0 fs, B=1 T, and (d) τ=3.0 fs, B=10 T. Note the difference in magnitudes for τ=1.6 fs and τ=3.0 fs. The above results refer to very narrow Landau levels, disregarding broadening due to electron scattering and the e-e interaction, see Section IV.

seconds or picoseconds but there is damping of the motion due to the light emission in a long time scale. The results shown in Figs. 2 and 3 refer to very narrow Landau levels, disregarding broadening due to electron scattering and the electron-electron (e-e) interaction, see Sec. IV.

We can draw the following qualitative conclusions from Figs. 2 and 3. First, for small magnetic fields B the period of oscillations is longer than for large fields, which is related to the basic frequency Ω. Second, irrespective of the variation of Ω with B, for small fields the oscillations are dominated by the low (cyclotron) frequency, while at stronger B the high (ZB) frequency dominates. Finally, comparing the magnitudes of dipole moment or emitted electric field for τ=1.6 fs with the corresponding values for τ=3.0 fs we observe that the amplitude of oscillations depends very strongly on the duration τ of the pulse.

To analyze these effects quantitatively we collected in Table I the coefficients b_{-1j} of Eq. (14), used for the calculation of electric field in Eq. (16). The results presented in Table I show that for fixed B and τ=1.6 fs the coefficients b_{-1-2} and b_{-10} are nearly three orders of magnitude larger than those for τ=3.0 fs. We also note that, for B=1 T, all b_{-1j} are nearly identical, while for B=40 T there are visible differences between various b_{-1j}. This difference is a factor of 3 for τ=1.6 fs, while for τ=3.0 fs the coefficient b_{-21} is two orders of magnitude larger than b_{-1-2}. This explains the dominance of the interband ZB frequency for large B in Figs. 2 and 3. The conclusion from this analysis is that the optimum conditions for observing the ZB, i.e. the packet motion with both interband and intraband frequencies, is the regime of magnetic fields of a few Tesla, since in this regime the two kinds of motion exist with comparable weights. One should note that the coefficients b_{-1j}, as defined in Eq. (11), are closely related to the coefficients c_{-1j} in the perturbation series, see Eqs. (9) and (14). A practical lower limit for magnetic fields is the condition that an energy distance between LLs should be larger than the widths Γ_L of LLs in graphene. According to Ref. 43 one observes resonant magneto-optical transitions, both interband and intraband, in graphene beginning with a magnetic field of $B\approx0.4$ T. Thus $B\approx0.5$ T

TABLE I. Coefficients b_{-1j} for the electric field in Eq. (16) for different pulse durations τ and various magnetic fields B.

τ (fs)	B (T)	b_{-1-2}	b_{-10}	b_{-12}
1.6	1	2.07×10^{-2}	2.09×10^{-2}	2.18×10^{-2}
	10	2.10×10^{-2}	2.26×10^{-2}	3.20×10^{-2}
	40	2.20×10^{-2}	2.84×10^{-2}	6.96×10^{-2}
3.0	1	1.52×10^{-5}	1.65×10^{-5}	2.45×10^{-5}
	10	1.76×10^{-5}	3.22×10^{-5}	1.89×10^{-4}
	40	2.63×10^{-5}	1.13×10^{-4}	2.74×10^{-3}

seems to be the lowest possible magnetic field suitable for the experiment described above. The Landau level broadening and its effect on ZB are discussed in the next section.

Comparing Figs. 2 and 3 for fixed τ one observes a strong dependence of the dipole moment on the magnetic field, while the radiated electric field depends only weakly on B. The reason is that the electric field of Eq. (16) is multiplied by a factor $d_0\Omega^2$. Because $d_0=-eL\zeta$, $\zeta\propto L$, and $\Omega=\sqrt{2u/L}$, the product $d_0\Omega^2$ does not depend on B. On the other hand, $d_0\propto L^2\propto B^{-1}$, and the dipole moment $\boldsymbol{D}(t)$ depends strongly on B. Therefore, the electric field of the emitted electromagnetic wave (and the radiated power) does not change significantly with the magnetic field intensity, it depends on B only via coefficients b_{-1j}, see Table I.

For $B=1$ T, the basic frequency Ω is 5.41×10^{13} s^{-1}, which corresponds to $f_\Omega=\Omega/(2\pi)=8.61$ THz. The cyclotron frequency is $f_c=3.53$ THz, while the ZB frequency is $f_Z=20.8$ THz. All the three frequencies are within the range of currently available THz photoconductive antennas, see e.g. Ref. 44, and it should be possible to detect the emitted field experimentally. In contrast, for $B=40$ T the corresponding frequencies are $f_\Omega=54.5$ THz, $f_c=22.3$ THz, and $f_Z=131$ THz, and they are more difficult to detect. This is the other reason for using low-magnetic fields in the experiment.

IV. ZB IN REAL SAMPLES

In the previous section we considered an idealized case of very narrow Landau levels in graphene. In real samples additional effects occur and their presence affects the motion of the wave packet. Two effects may play a role in the proposed experiment: the e-e interaction[45] and the presence of disorder.[46,47] The scanning tunnelling spectroscopy results of Ref. 45 indicate that the e-e interaction leads to a Lorentzian shape of DOS of the Landau levels and it opens an energy gap between the electrons and holes. Thus the massless Dirac fermions acquire a small nonzero mass. As shown in the numerical simulations of Ref. 46, the presence of disorder changes the shape of DOS from Lorentzian to Gaussian peaks. Additionally, the disorder potential may change the position of the Fermi level within sample.

The band-gap caused by the e-e interaction is of the order of 10 meV,[45] so at a magnetic field of $B=1$ T it is much smaller than the basic energy $\hbar\Omega\approx36$ meV. In this case the energy spectrum of graphene in a magnetic field is described by an analogue of the Dirac equation, whose energy levels and eigenfunctions are well known. The trembling motion of the packet will not change qualitatively, as compared to the above description, but it will oscillate with the interband frequency $\tilde{\Omega}=\sqrt{\Omega^2+E_{\rm gap}^2/\hbar^2}$, and all frequencies will have slightly different values than those calculated in the gapless model.

On the other hand, the broadening of the Landau levels may strongly influence the trembling motion of the wave packet. To analyze the overall impact of all the effects leading to the level broadening: disorder, e-e interaction, electron-phonon scattering, etc., we assume finite widths of all energy levels, characterized by broadening parameters Γ_n.

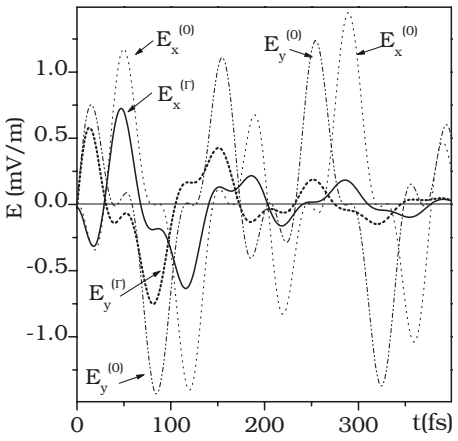

FIG. 4. Calculated electric fields $E_x(t)$ and $E_y(t)$ emitted by one trembling electron during the first 400 fs after the laser pulse. Pulse parameters: intensity 1×10^9 W/cm^2, $\tau=1.6$ fs, magnetic field $B=1$ T. Bold lines—electric fields for broadened Landau levels described by Lorentzian line shapes with experimental values of Γ_n (see text). Thinner lines—electric fields for delta-like Landau levels. The latter results are the same as those shown in Fig. 3(a).

We treat Γ_n as phenomenological quantities determined experimentally and including all scattering mechanisms existing in real samples. We approximate the broadening of DOS by a Lorentzian line shape[45] irrespective of the detailed scattering mechanism.[46] In this approximation the Landau energies E_n are replaced by complex energies $\tilde{E}_n=E_n+i\Gamma_n$. After the replacement the dipole moment of Eq. (13) changes to

$$D_y^\Gamma(t)\simeq \text{const}+eL\sum_{j=0,\pm2} c_{-1j}^1 a_{-1j}^y e^{i\omega_{-1j}t-\Gamma_j t}+\text{H.c.}+\ \ldots\ , \tag{17}$$

which leads to [cf. Eq. (15)]

$$D_y^\Gamma(t)=d_0\left[-\frac{b_{-10}}{2}\sin(\omega_0^c t)e^{-\Gamma_0 t}+B^- b_{-12}\sin(\omega_1^Z t)e^{-\Gamma_{+2}t}\right.$$
$$\left.+B^+ b_{-1-2}\sin(\omega_1^c t)e^{-\Gamma_{-2}t}\right],$$

$$D_x^\Gamma(t)=d_0\left[\frac{b_{-10}}{2}\cos(\omega_0^c t)e^{-\Gamma_0 t}+B^- b_{-12}\text{c os}(\omega_1^Z t)e^{-\Gamma_{+2}t}\right.$$
$$\left.-B^+ b_{-1-2}\cos(\omega_1^c t)e^{-\Gamma_{-2}t}\right]. \tag{18}$$

As to the numerical values of Γ_n, we take after Ref. 45 $\Gamma_{\pm2}=5.1$ meV. For the state $n=0$ we use $\Gamma_0=4.3$ meV (Ref. 46), which corresponds to the disorder potential $V_g=120$ meV.[47] These values are similar to the line widths of $\Gamma_n=7$ meV measured at $B=1$ T in far infrared transmission experiments,[48] and $\Gamma_n=1.6$ meV determined by the Quantum Hall Effect at $B\sim40$ T.[49]

The electric field $\boldsymbol{E}(t)$ is calculated, as before, as a second time derivative of $\boldsymbol{D}^\Gamma(t)$, see Eq. (15). In Fig. 4 we plot the electric field emitted by an oscillating electron within the first 400 fs of motion after the laser shot of the width τ

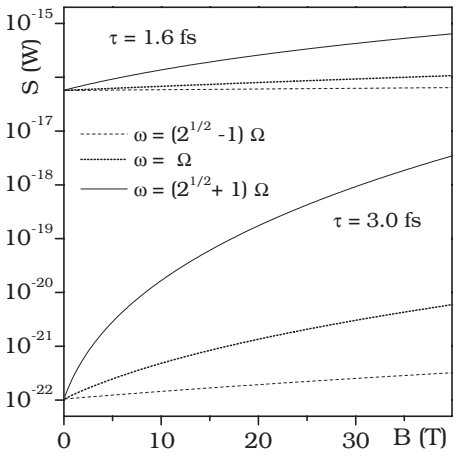

FIG. 5. Intensity of three emission lines versus magnetic field for two laser pulses of different durations τ.

$=1.6$ fs in a magnetic field $B=1$ T. The two bold lines describe calculated electric fields $E_x(t)$ and $E_y(t)$ for the Landau levels having the broadening parameters Γ_n indicated above. The two thinner lines show the electric fields calculated without damping ($\Gamma_n=0$), see Eq. (15) and Fig. 3(a). Within the first 50 fs of motion the electric fields emitted in the two cases are similar, but later the damping of the emitted fields for broadened levels is visible. After around 400 fs the trembling motion in real case disappears. It can be seen that the maxima of oscillations for the damped ZB motion coincide with the undamped ones. The general conclusion from Fig. 4 is that the existence of disorder, many-body effects or other scattering mechanisms changes the persistent ZB motion to a decaying one, within the characteristic lifetimes for these processes: $\tau_n=1/\Gamma_n \approx 130$ fs. Nevertheless, since the parameters Γ_n used in the calculations correspond to the measured lifetimes in real graphene samples, it follows that the broadening of the Landau levels does not prevent the existence of ZB. Clearly, a lower disorder in better samples will result in longer decay times for ZB.

V. TIME-RESOLVED LUMINESCENCE

Knowing the electric field emitted by an oscillating dipole we can calculate the intensity of radiated light. If $\mathcal{E}(t)$ is given by a sum of cosine (or sine) functions: $\mathcal{E}(t)=\Sigma_j f_j \cos(\omega_j t)$, the emitted power averaged over a long time is $\bar{P}=(1/2)\Sigma_j |f_j|^2$. The total power S passing through a closed spherical surface at a distance R from the sample can be calculated integrating $\bar{P}$ over the enclosing surface. Using Eq. (16) and the above formula we find

$$S=\frac{d_0^2\Omega^4}{96\pi\epsilon_0 c^3}(4|b_{-10}|^2+|b_{-12}|^2+|b_{-1-2}|^2), \tag{19}$$

which is the Larmor formula for our problem. The emitted spectrum S consists of three lines of different intensities having the frequencies $\omega=\Omega$, $\omega=(\sqrt{2}+1)\Omega$, and $\omega=(\sqrt{2}-1)\Omega$. The existence of lines with interband frequencies is the signature of Zitterbewegung in this system. In Fig. 5 we plot the relative light intensities for different emission lines versus magnetic field B on the logarithmic scale. The upper curves correspond to $\tau=1.6$ fs, the lower ones to $\tau=3.0$ fs. In both cases the intensities depend on magnetic field, this dependence is most pronounced for the ZB frequencies. However, for $\tau=1.6$ fs the dependence of intensities on the magnetic field is much weaker than for $\tau=3.0$ fs. At high B the spectrum is dominated by the ZB frequencies. It should be noted that the intensity of radiation is proportional to Ω^4 and to $\zeta^2 \propto \mathcal{E}_0^2$, as for the Thompson scattering.

To observe the motion of electron represented by a wave packet one can use the time-resolved luminescence.[50–52] In this technique, the electric field $\mathcal{E}(t)$ of the light emitted by a sample is transmitted through two filters: a time gate $B(t,T)$

$$B(t,T)=\exp(-\Gamma|t-T|), \tag{20}$$

and a frequency filter $H(t,\omega_F)$

$$H(\omega,\omega_F)=\frac{\gamma^2}{\gamma^2+(\omega-\omega_F)^2}. \tag{21}$$

The time gate lets the field pass for $T-\Gamma/2<t<T+\Gamma/2$, where Γ is the gate's parameter describing the width of the window, and T is the center of the window. The frequency filter selects frequencies close to ω_F with the resolution γ. The transmitted field is

$$\mathcal{E}_{HB}(t)=\int_{-\infty}^{t} H(t-t',\omega_F)B(t',T)\mathcal{E}(t')dt', \tag{22}$$

where $H(t,\omega_F)$ is the Fourier transform of $H(\omega,\omega_F)$. The time-dependent spectrum of $\mathcal{E}(t)$ is

$$S(T,\omega_F)=\int dA \int_{-\infty}^{\infty} |\mathcal{E}_{HB}(t)|^2 dt, \tag{23}$$

where the first integration is over the sphere of radius R enclosing the sample. For $\mathcal{E}(t)$ given by Eq. (16) we obtain

$$S(T,\omega_F)=M\sum_{\alpha,\beta,r} b_\alpha^r b_\beta^r e^{-i(\omega_\alpha-\omega_\beta)T}G(\alpha,\beta), \tag{24}$$

where M is a constant and $\alpha,\beta=(n,j,s)$. The summation is restricted to $n=-1$, $j=0,\pm 2$, and $s=\pm 1$. The index $r=x,y$, and we denote $\omega_\alpha,\omega_\beta \equiv s\omega_{nj}$. Factors b_α^r and b_β^r are the coefficients in front of trigonometric functions in Eq. (16). We have $b_{-10}^y=b_{-10}/2$, $b_{-12}^y=b_{-12}/4$, and $b_{-1-2}^y=-b_{-1-2}/4$. Similarly $b_{-10}^x=-b_{-10}/2$, $b_{-12}^x=b_{-12}/4$, and $b_{-1-2}^x=b_{-1-2}/4$. The analytical function $G(\alpha,\beta)$ is defined by Eq. (17) of Ref. 51.

In Fig. 6 we show the calculated time-dependent spectrum of ZB oscillations for the following parameters: laser pulse width $\tau=1.6$ fs, laser wavelength $\lambda_L=650$ nm, magnetic field $B=1$ T, frequency filter $\gamma=3$ cm^{-1}, and the gate width $\Gamma=1000$ cm^{-1}. Three curves correspond to frequency spectrum observed at three gate opening times T. If follows from Eq. (24) and from the selection rules for j, see Eq. (10), that the time-dependent spectrum $S(T,\omega_F)$ has maxima at the frequencies: $\omega=\omega_c$, $\omega=\Omega$, and $\omega=\omega_Z$. Because of finite resolutions of the time gate and the frequency filter, the maxima for $\omega=\omega_c$ and $\omega=\Omega$ form one unresolved peak.

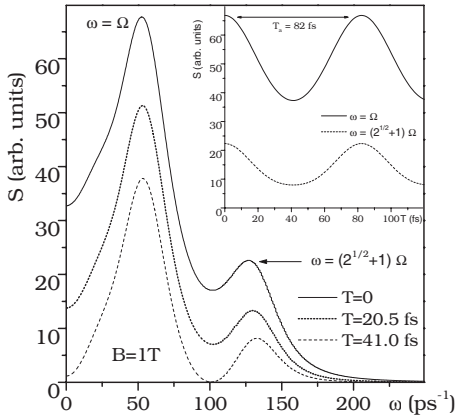

FIG. 6. Calculated power spectra of the emitted light for different opening gate times T. For the assumed resolutions $\gamma=3$ cm^{-1} and $\Gamma=1000$ cm^{-1} the peaks at $\omega=\Omega$ and $\omega=(\sqrt{2}-1)\Omega$ are not resolved. Inset: Intensity of two peaks: $\omega=\Omega$ and $\omega=(\sqrt{2}+1)\Omega$ versus gate time T. Repetition of oscillation pattern occurs after $T_a=\sqrt{2}\Omega=82.2$ fs for $B=1$ T.

Changing the gate opening time T one should observe different frequency spectra. The spectrum repeats its pattern after $T_a=2\pi/\omega_a=82.2$ fs, where $\omega_a=\omega_{-10}-\omega_{-1-2}=\sqrt{2}\Omega$. To illustrate this time dependence we plot in the inset of Fig. 6 intensities of the emitted radiation for two frequencies: $\omega=\Omega$ and $\omega=\Omega_Z$ versus gate's opening time T. We see that, for both maxima, the intensities oscillate with the period T_a. The oscillating pattern of $S(T,\omega_F)$ is also the signature of Zitterbewegung.

VI. DISCUSSION

In Sec. II we assumed that the Fermi level in monolayer graphene coincides with the Landau level $n=-2$ and considered the initial electron in the state $n=-1$, see Fig. 1. This means that, before the electron reacts to a short laser pulse, it must be pumped to the state $n=-1$ from lower Landau levels. A conventional light source is suitable for such pumping but, in order to achieve high intensities of the emitted lines, one should use a laser pump in resonance with $\hbar\omega=E_{-1}-E_{-2}$ energy. It should be emphasized that the upper component of the state $n=-1$ in a magnetic field is described by the Gaussian wave function in space, but, since it is an eigenstate, it does not have a time dependence. The decisive factor is the subsequent laser pulse which excites a series of electron eigenstates.

The results described by Eq. (16) are obtained for *one* electron. The population of the Landau level is eB/h and the total intensity of radiation is obtained by adding the contributions from all electrons in the initial $n=-1$ level. In our proposition we select the initial electron state $n=-1$ for several reasons. Due to the selection rules $\Delta|j|=\pm 1$ there exist three frequencies ω_{-1j} contributing to the electron motion. If the state $n=0$ were selected, there would be only two nonvanishing matrix elements $y_{0,-1}=y_{0,+1}$ corresponding to the same frequency Ω, see Fig. 1. Assuming the Fermi energy at the $n=-2$ LL and supposing, in consequence, the state $n=-2$ to be roughly half filled, we avoid the Pauli exclusion principle in the calculation of the dipole matrix elements. Therefore, one-particle formalism of ZB calculation can be applied, see Refs. 33 and 34. The presence of a magnetic field is essential for a successful experiment since, as we said above, in the absence of magnetic field the ZB oscillations have a transient character with the decay time of tenths of femtoseconds[12,16,18] and the detection of such oscillations is difficult. However, as we showed in Sec. IV, the broadening of Landau levels also leads to a transient character of ZB. In high-quality graphene samples with small disorder the electron ZB should last longer after the laser pulse.

From the early eighties, short laser pulses were used in quantum chemistry to excite wave packets in molecules.[53] After a laser shot, the nonstationary wave packet evolves in time and its motion is measured in many ways: absorption, luminescence, Raman scattering, etc., using the so called pump and probe method. The experiment proposed here is in principle similar to these techniques. Our additional requirement is the necessity to use monocycle or submonocycle laser pulses in order to excite the electron packet with both positive and negative energies.[31]

In the nineties, the Bloch oscillations were observed in superlattices in a static electric field. In these experiments the electric field creates a set of discrete levels [Wannier-Stark ladder (WSL)]. Then, a short laser pulse creates a wave packet consisting of many discrete states and an oscillating dipole moment appears. The oscillations of the dipole moment were measured either by detection of THz radiation,[54] or by measuring change in the positions of WSL energies in pump and probe experiments.[55] There exist several similarities between the Bloch oscillator experiment and our proposition. In both cases the system is quantized by an external field, the laser pulse creates an electron wave packet consisting of many discrete levels, and the oscillations of the wave packet lead to the time-dependent dipole moment that can be observed experimentally. The main difference is, again, that in order to observe ZB one needs to create an electron packet having both positive and negative energy states. Finally, similar techniques to the one proposed here were applied to observe a coherent emission from double-well systems.[56,57]

In our treatment we used the first order time-dependent perturbation theory, see Eq. (12). For very strong electric fields this approach may be insufficient. However, the fast decrease in b_{-1j} coefficients with increasing pulse width τ assures in practice the validity of the perturbation expansion.

It was shown in the previous work on ZB that its existence is related to a nonzero momentum of the electron.[6,12] In our gauge for $\boldsymbol{A}$, the initial electron state has an initial momentum k_x. A laser pulse $\hat{W}(t)$ creates the state with nonzero momentum also in the y direction. Direct calculations show that at $t=0$ the average momentum is $\langle\hat{p}_i\rangle=\langle\Psi(0)|(\hbar/i)(\partial/\partial x_i)|\Psi(0)\rangle$ which gives $\langle\hat{p}_y\rangle=2\zeta\hbar/L$ and $\langle\hat{p}_x\rangle=k_x$. These results are obtained in the lowest order in $\mathcal{E}_0$. The asymmetry between x and y directions follows from the electric field $\mathcal{E}$ directed parallel to the y axis.

As we said above, several conditions should be met in order to observe the ZB. In our understanding, all these conditions can be fulfilled: p-doped monolayer graphene, ultrashort pulse of the required intensity, detection of the emit-

ted electric field in the 3–21 THz range, or an observation of the time resolved spectra. It should be possible to satisfy these conditions in a single experiment.

VII. SUMMARY

To summarize, we proposed and described a possible method to observe the trembling motion of electrons in graphene in a magnetic field. The central point is that we did not assume anything about the shape of the initial electron wave packet. We calculated the time-dependent dipole moment induced by an ultra-short laser pulse. For electrons located initially in the $n=-1$ state the induced dipole moment oscillates with three frequencies, of which the frequency $\omega_Z=(\sqrt{2}+1)\Omega$ is the signature of Zitterbewegung. A possibility of performing such an experiment and detecting the ω_Z frequency are discussed and it appears that the current experimental techniques are sufficient for a successful observation of ZB in high-quality graphene samples.

ACKNOWLEDGMENTS

This work was supported in part by The Polish Ministry of Science and Higher Education through Laboratory of Physical Foundations of Information Processing.

APPENDIX

It is well known that in the Brillouin zone of monolayer graphene there exist two inequivalent minimum points K_1 and K_2.[37,58] Above we calculated contributions from an electron at the point K_1 defined by Hamiltonian (4). The question arises: what is the contribution of an electron at the point K_2? To elucidate this issue we consider the Hamiltonian for electrons at the K_2 point of BZ[37,58]

$$\hat{H}_2 = \hbar\Omega \begin{pmatrix} 0 & \hat{a}^+ \\ \hat{a} & 0 \end{pmatrix}. \tag{A1}$$

Comparing Eq. (A1) with Eq. (4) it is seen that $\hat{H}_2=-\hat{H}_1^T$. The eigenenergies of both Hamiltonians are the same, but the eigenstates of $\hat{H}_2$ are

$$\chi_n(\boldsymbol{r}) = \frac{e^{ik_x x}}{\sqrt{4\pi}} \begin{pmatrix} \phi_{|n|}(\xi) \\ \mathrm{sgn}(n)\phi_{|n|-1}(\xi) \end{pmatrix}, \tag{A2}$$

which differs from $\psi(\boldsymbol{r})$ of Eq. (2) by an exchange of the upper and lower components and by the change in sign of $\phi_{|n|-1}(\xi)$ state. The matrix elements are $\langle\psi|y|\psi\rangle=\langle\chi|y|\chi\rangle$, so both Hamiltonians give the same selection rules. The perturbed wave function $\Upsilon(\boldsymbol{r},t)$ for the electron at the K_2 point is [see Eq. (12)]

$$\Upsilon_{-1}(t) \simeq e^{-iE_{-1}t/\hbar}\chi_{-1} + \sum_{j=0,\pm 2} c^1_{-1j} e^{-iE_j t/\hbar}\chi_j, \tag{A3}$$

with the same coefficients c_{-1j} as in Eq. (12). In consequence, the wave packet at $t=0$ for the electron at the K_1 point is [see Eq. (12)]

$$\Psi_{-1}(0) \simeq \psi_{-1} + \sum_{j=0,\pm 2} c^1_{-1j}\psi_j, \tag{A4}$$

while for the K_2 point the initial wave packet is

$$\Upsilon_{-1}(0) \simeq \chi_{-1} + \sum_{j=0,\pm 2} c^1_{-1j}\chi_j. \tag{A5}$$

Thus, the same laser shot creates two *different* electron wave packets at K_1 and K_2 points. This is in contrast to the assumption made in Ref. 15, where the same wave packet was assumed for both K_1 and K_2 points. The result of this assumption was a partial cancellation of one of the electric current components. This was unphysical since it violated the rotational symmetry of the x-y graphene plane. In the present approach, the two wave packets evolve according to *different* Hamiltonians. There is $\Psi_{-1}(t)=e^{-i\hat{H}_1 t/\hbar}\Psi_{-1}(0)$ and $\Upsilon_{-1}(t)=e^{-i\hat{H}_2 t/\hbar}\Upsilon_{-1}(0)$. A direct calculation shows that now the contributions to the electric current and dipole oscillations arising from electrons excited at the two nonequivalent points K_1 and K_2 are equal.

*tomasz.rusin@centertel.pl

[1] E. Schrodinger, Sitzungsber. Preuss. Akad. Wiss., Phys. Math. Kl. **24**, 418 (1930).
[2] W. Zawadzki, in *Optical Properties of Solids*, edited by E. D. Haidemenakis (Gordon and Breach, New York, 1970), p. 179.
[3] W. Zawadzki, in *High Magnetic Fields in the Physics of Semiconductors II*, edited by G. Landwehr and W. Ossau (World Scientific, Singapore, 1997), p. 755.
[4] W. Zawadzki, Phys. Rev. B **72**, 085217 (2005).
[5] F. Cannata, L. Ferrari, and G. Russo, Solid State Commun. **74**, 309 (1990); L. Ferrari and G. Russo, Phys. Rev. B **42**, 7454 (1990).
[6] J. Schliemann, D. Loss, and R. M. Westervelt, Phys. Rev. Lett. **94**, 206801 (2005).
[7] W. Zawadzki, Phys. Rev. B **74**, 205439 (2006).
[8] M. I. Katsnelson, Eur. Phys. J. B **51**, 157 (2006).
[9] R. Winkler, U. Zulicke, and J. Bolte, Phys. Rev. B **75**, 205314 (2007).
[10] M. Auslender and M. I. Katsnelson, Phys. Rev. B **76**, 235425 (2007).
[11] T. M. Rusin and W. Zawadzki, J. Phys.: Condens. Matter **19**, 136219 (2007).
[12] T. M. Rusin and W. Zawadzki, Phys. Rev. B **76**, 195439 (2007).
[13] B. Trauzettel, Y. M. Blanter, and A. F. Morpurgo, Phys. Rev. B **75**, 035305 (2007).
[14] U. Zulicke, J. Bolte, and R. Winkler, New J. Phys. **9**, 355

(2007).
[15] T. M. Rusin and W. Zawadzki, Phys. Rev. B **78**, 125419 (2008).
[16] W. Zawadzki and T. M. Rusin, J. Phys.: Condens. Matter **20**, 454208 (2008).
[17] R. Englman and T. Vertesi, Phys. Rev. B **78**, 205311 (2008).
[18] V. Y. Demikhovskii, G. M. Maksimova, and E. V. Frolova, Phys. Rev. B **78**, 115401 (2008).
[19] J. Cserti and G. David, Phys. Rev. B **74**, 172305 (2006).
[20] L. Lamata, J. Leon, T. Schatz, and E. Solano, Phys. Rev. Lett. **98**, 253005 (2007).
[21] J. Y. Vaishnav and C. W. Clark, Phys. Rev. Lett. **100**, 153002 (2008).
[22] X. Zhang, Phys. Rev. Lett. **100**, 113903 (2008).
[23] M. Merkl, F. E. Zimmer, G. Juzeliunas, and P. Ohberg, Europhys. Lett. **83**, 54002 (2008).
[24] A. Bermudez, M. A. Martin-Delgado, and A. Luis, Phys. Rev. A **77**, 033832 (2008).
[25] J. C. Martinez, M. B. A. Jalil, and S. G. Tan, arXiv:0806.0222 (unpublished).
[26] B. Dora, K. Ziegler, P. Thalmeier, and M. Nakamura, Phys. Rev. Lett. **102**, 036803 (2009).
[27] X. Zhang and Z. Liu, Phys. Rev. Lett. **101**, 264303 (2008).
[28] J. A. Lock, Am. J. Phys. **47**, 797 (1979).
[29] J. Schliemann, New J. Phys. **10**, 043024 (2008).
[30] K. Huang, Am. J. Phys. **20**, 479 (1952).
[31] W. Greiner, *Relativistic Quantum Mechanics* (Springer, Berlin, 1994).
[32] J. D. Bjorken and S. D. Drell, *Relativistic Quantum Mechanics* (McGraw-Hill, New York, 1964).
[33] P. Krekora, Q. Su, and R. Grobe, Phys. Rev. Lett. **93**, 043004 (2004).
[34] Z. Y. Wang and C. D. Xiong, Phys. Rev. A **77**, 045402 (2008).
[35] K. S. Novoselov, A. K. Geim, S. V. Morozov, D. Jiang, Y. Zhang, S. V. Dubonos, I. V. Grigorieva, and A. A. Firsov, Science **306**, 666 (2004).
[36] K. S. Novoselov, A. K. Geim, S. V. Morozov, D. Jiang, M. I. Katsnelson, I. V. Grigorieva, S. V. Dubonos, and A. A. Firsov, Nature (London) **438**, 197 (2005).
[37] V. P. Gusynin, S. G. Sharapov, and J. P. Carbotte, Int. J. Mod. Phys. B **21**, 4611 (2007).
[38] D. Bohm, *Quantum Theory* (Prentice-Hall, New York, 1952).
[39] J. D. Jackson, *Classical Electrodynamics* (Wiley, New York, 1975).
[40] L. D. Landau and E. M. Lifschitz, *Quantum Mechanics: Non-Relativistic Theory* (Oxford University Press, Oxford, 1977).
[41] M. Y. Shverdin, D. R. Walker, D. D. Yavuz, G. Y. Yin, and S. E. Harris, Phys. Rev. Lett. **94**, 033904 (2005).
[42] A. L. Cavalieri, E. Goulielmakis, B. Horvath, W. Helml, M. Schultze, M. Fiess, V. Pervak, L. Veisz, V. S. Yakovlev, M. Uiberacker, A. Apolonski, F. Krausz, and R. Kienberger, New J. Phys. **9**, 242 (2007).
[43] M. L. Sadowski, G. Martinez, M. Potemski, C. Berger, and W. A. de Heer, Phys. Rev. Lett. **97**, 266405 (2006).
[44] S. Kono, M. Tani, and K. Sakai, Appl. Phys. Lett. **79**, 898 (2001).
[45] G. Li, A. Luican, and E. Y. Andrei, Phys. Rev. Lett. **102**, 176804 (2009).
[46] W. Zhu, Q. W. Shi, X. R. Wang, J. Chen, J. L. Yang, and J. G. Hou, Phys. Rev. Lett. **102**, 056803 (2009).
[47] C. Stampfer, J. Guttinger, S. Hellmuller, F. Molitor, K. Ensslin, and T. Ihn, Phys. Rev. Lett. **102**, 056403 (2009).
[48] M. Orlita, C. Faugeras, P. Plochocka, P. Neugebauer, G. Martinez, D. K. Maude, A. L. Barra, M. Sprinkle, C. Berger, W. A. de Heer, and M. Potemski, Phys. Rev. Lett. **101**, 267601 (2008).
[49] Y. Zhang, Z. Jiang, J. P. Small, M. S. Purewal, Y. W. Tan, M. Fazlollahi, J. D. Chudow, J. A. Jaszczak, H. L. Stormer, and P. Kim, Phys. Rev. Lett. **96**, 136806 (2006).
[50] J. H. Eberly and K. Wodkiewicz, J. Opt. Soc. Am. **67**, 1252 (1977).
[51] P. Kowalczyk, C. Radzewicz, J. Mostowski, and I. A. Walmsley, Phys. Rev. A **42**, 5622 (1990).
[52] T. J. Dunn, J. N. Sweetser, I. A. Walmsley, and C. Radzewicz, Phys. Rev. Lett. **70**, 3388 (1993).
[53] A. Zewail, *Nobel Lecture* (1999); available on http://nobelprize.org/nobel_prizes/chemistry/laureates/1999/zewail-lecture.pdf.
[54] R. Martini, G. Klose, H. G. Roskos, H. Kurz, H. T. Grahn, and R. Hey, Phys. Rev. B **54**, R14325 (1996).
[55] V. G. Lyssenko, G. Valusis, F. Loser, T. Hasche, K. Leo, M. M. Dignam, and K. Kohler, Phys. Rev. Lett. **79**, 301 (1997).
[56] S. Luryi, IEEE J. Quantum Electron. **27**, 54 (1991).
[57] H. G. Roskos, M. C. Nuss, J. Shah, K. Leo, D. A. B. Miller, A. M. Fox, S. Schmitt-Rink, and K. Kohler, Phys. Rev. Lett. **68**, 2216 (1992).
[58] C. Bena and G. Montambaux, arXiv:0712.0765, New J. Phys. (to be published).